
Sym-Q: Adaptive Symbolic Regression via Sequential Decision-Making

Yuan Tian¹ Wenqi Zhou¹ Hao Dong² David S. Kammer¹ Olga Fink²

Abstract

Symbolic regression holds great potential for uncovering underlying mathematical and physical relationships from empirical data. While existing transformer-based models have recently achieved significant success in this domain, they face challenges in terms of generalizability and adaptability. Typically, in cases where the output expressions do not adequately fit experimental data, the models lack efficient mechanisms to adapt or modify the expression. This inflexibility hinders their application in real-world scenarios, particularly in discovering unknown physical or biological relationships. Inspired by how human experts refine and adapt expressions, we introduce Symbolic Q-network (Sym-Q), a novel reinforcement learning-based model that redefines symbolic regression as a sequential decision-making task. Sym-Q leverages supervised demonstrations and refines expressions based on reward signals indicating the quality of fitting precision. Its distinctive ability to manage the complexity of expression trees and perform precise step-wise updates significantly enhances flexibility and efficiency. Our results demonstrate that Sym-Q excels not only in recovering underlying mathematical structures but also uniquely learns to efficiently refine the output expression based on reward signals, thereby discovering underlying expressions. Sym-Q paves the way for more intuitive and impactful discoveries in physical science, marking a substantial advancement in the field of symbolic regression.

1. Introduction

Symbolic regression is a powerful form of regression analysis that searches the space of mathematical expressions to find the expression that best fits a given dataset. Unlike traditional regression models that fit data to pre-specified equations, symbolic regression is capable of discovering

¹ETH Zürich ²EPFL. Correspondence to: Olga Fink <olga.fink@epfl.ch>.

Preprint. Under review.

the underlying equations or relationships between variables. This capability can lead to a deeper understanding of the inherent structure and dynamics of the data and is particularly important in fields where the relationships between variables are complex and not well understood, as it provides a tool to uncover the form of the relationship without prior assumptions. Recently, symbolic regression has been instrumental in uncovering new relationships, such as astrophysical scaling relations (Wadekar et al., 2022) and analytical models of exoplanet transit spectroscopy (Matchev et al., 2022). However, a significant challenge in symbolic regression is its inherent complexity. This complexity grows rapidly with the length of the symbolic expressions, making it a computationally demanding NP-hard problem (Li et al., 2022).

Symbolic regression has primarily been explored through two approaches: online search methods like Genetic programming (GP) and transformer-based models trained with extensive data. GP, a leading online search method (Forrest, 1993; Schmidt & Lipson, 2009; Augusto & Barbosa, 2000; Gustafson et al., 2005; Bladdek & Krawiec, 2019), iteratively evolves each generation of mathematical expressions to match the observation points through selection, crossover, and mutation. Besides, previous reinforcement learning-based (RL) methods, like deep symbolic optimization (DSO) (Petersen et al., 2019), optimize expressions based on reward signals during online search. Some recent methods even combine GP with RL, leveraging the advantages of both approaches (Mundhenk et al., 2021). However, despite their effectiveness, these online search methods treat symbolic regression as an instance-based problem, requiring model training or searching from scratch for each case, leading to inefficiency and high computational demands.

Building upon the advancements facilitated by large-scale language models (Vaswani et al., 2017), recent efforts in symbolic regression have focused on using transformer-based models, which are trained on extensive datasets (Li et al., 2022; Vastl et al., 2022; Kamienny et al., 2022; Bendinelli et al., 2023). Although transformer-based models have recently achieved significant success in symbolic regression, showing considerable capability in finding the underlying equations for many cases, they still face challenges in generalizability and adaptability. These models lack efficiency in adapting their output expressions after training. This lack of flexibility severely constrains their

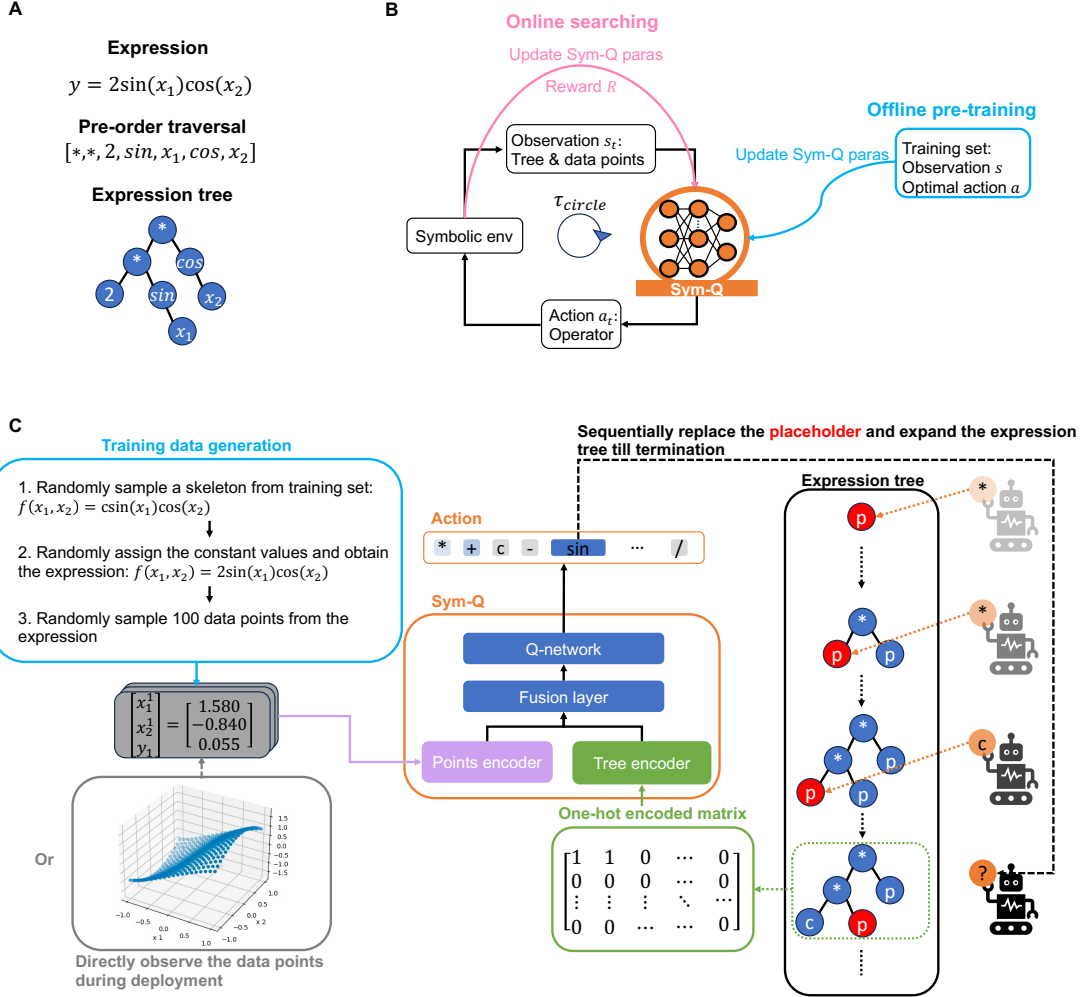


Figure 1. Overview of the proposed framework. **A**. The expression and its corresponding expression tree. **B**. The proposed Sym-Q agent supports both offline training with ground truth human knowledge and online searching with reward signals. τ_{circle} represents the agent trajectories within the symbolic environment. **C**. The Sym-Q architecture and step-wise decision-making mechanism.

utility in practical applications, as it requires the training dataset to comprehensively cover relevant expressions. Such rigidity is particularly limiting in fields like physics or biology, where the ability to uncover new relationships hinges on the model’s flexibility and adaptability.

Transformer-based models in symbolic regression can sometimes produce near-correct expressions with minor errors, like a single incorrect operator. Rather than re-optimizing the entire sequence from beginning, an efficient model be able to pinpoint and correct just the erroneous element.

To address this challenge, we introduce a novel approach by conceptualizing symbolic regression as a Markov decision process (MDP) for the first time. In our new framework, the model assesses the current expression tree and observed data at each step to choose an action that maximizes cumulative rewards like the coefficient of determination (R^2) (Glantz

et al., 2001). This reformulation transforms the large action space (m^l , where m is the number of total possible operations for each step and l is the maximum decision depth) into a more manageable scope, reducing the actions per step to just the number of total possible operations m . Consequently, this novel formulation facilitates efficient, step-wise updating and adapting of the expression (Tian et al., 2020).

Under this formulation, in this work, we introduce Symbolic Q-network (Sym-Q), a novel RL-based method for symbolic regression as illustrated in Figure 1. This approach, under the MDP formulation, innovatively combines online RL techniques with pretrained transformer-based models. Sym-Q is the first approach to employ sequential decision-making for generating and refining expression trees, representing a pioneering step in the intersection of RL and symbolic regression. It leverages the strengths of both RL and advanced transformer models to iteratively explore and optimize the

space of mathematical expressions. The key contributions of our study are threefold:

- We reformulate symbolic regression as a sequential decision-making process, demonstrating its effectiveness.
- Building upon this new problem formulation, we propose the Sym-Q model. Sym-Q is trained via offline RL and is also compatible with online RL methods, enabling efficient refinement and adaptation of output expressions in response to reward signals.
- Empirically, Sym-Q outperforms current state-of-the-art transformer-based models, particularly in recovering expression structures and refining output expressions based on rewards. We provide an in-depth analysis of the model’s performance, offering insights for future training data design and method improvements. Our source code will be publicly available.

2. Related works

The field of symbolic regression has been primarily explored in two methodological trajectories: online searching methods, and transformer-based models. Genetic programming-based approaches are the most widely used in the online searching category and include many notable works such as (Forrest, 1993; Schmidt & Lipson, 2009; Augusto & Barbosa, 2000; Gustafson et al., 2005; Bladek & Krawiec, 2019). By far the most popular commercial software Eureqa (Dubčáková, 2011) is the most successful application based on GP methods.

Within the field of online search methods for symbolic regression, RL-based approaches represent a significant advancement (Petersen et al., 2019; Tenachi et al., 2023), as highlighted by Petersen et al. (2019) in their introduction of deep symbolic optimization (DSO). DSO employs a risk-seeking policy gradient to effectively train a recurrent neural network (RNN), which then generates a probability distribution over the space of mathematical expressions. Additionally, this field has witnessed the advent of diverse search methodologies, such as normalizing flows (Udrescu & Tegmark, 2020) and the combination of genetic programming with RL (Mundhenk et al., 2021), aiming to capitalize on the strengths of both. Despite their potential, these methods typically require searches or training for each instance from scratch, leading to computational challenges and stochastic variability.

The second methodological approach in symbolic regression focuses on transformer-based models trained on extensive datasets and has shown promise in identifying underlying equations in various scenarios. Recent works, including those by Li et al. (2022); Vastl et al. (2022); Kamienny et al. (2022); Bendinelli et al. (2023), demonstrate the effectiveness of transformer models in this field. Models like

NeSymReS (Biggio et al., 2021) and SymbolicGPT have pioneered the use of Set transformers (Devlin et al., 2018; Lee et al., 2019) and GPT frameworks (Valipour et al., 2021), respectively, for encoding observed data points and generating expressions. Li et al. (2022) introduce a novel approach employing PointMLP (Ma et al., 2022) for local and global feature extraction and a joint learning mechanism that combines supervised contrastive learning with the guidance of the preorder traversal of expression trees. Neural Symbolic Regression with Hypothesis (NSRwH) (Bendinelli et al., 2023) proposes the inclusion of assumptions about the ground truth expression structure in the prediction process. While Kamienny et al. (2022) proposes to directly output complete expressions, including constants, these mentioned models’ generally face limitations in adapting output expressions efficiently, which restricts their practical application in real-world scenarios. Notably, existing learning-based works, whether RL-based or transformer-based, do not facilitate step-wise updates and refinements, a gap that our approach aims to address.

3. Method

3.1. Overview

In this work, we propose Sym-Q, an RL-based method for addressing large-scale symbolic regression problems. The overview of the proposed Sym-Q is depicted in Figure 1. By reformulating symbolic regression as an MDP, the agent is trained to understand the observations and sequentially expand and refine the expression tree. As illustrated in Figure 1.B, Sym-Q is capable of learning from both optimal demonstrations, and sub-optimal reward signals. Initially, the agent is trained using the proposed offline RL method and can further refine its policy through our proposed off-policy RL method during online searching.

Figure 1.C details the decision-making process. At each time step, the agent observes the encoded data points and the encoded preceding expression tree. Utilizing this encoded information, the agent identifies the placeholder node (shown as red node in the tree) that needs to be replaced. Then the agent sequentially replaces the placeholders and expands the expression tree until termination. This process is performed 128 times using the beam search strategy, resulting in 128 distinct skeletons.

The final expression is then derived by applying the Broyden–Fletcher–Goldfarb–Shanno (BFGS) (Fletcher, 2000) optimization, focusing on the constant terms in the expressions. For detailed implementation, the pseudo-code of our deployment strategy is available in Appendix A.

3.2. Expression tree

An expression tree, as described by Hopcroft et al. (2006), is a structure where internal nodes symbolize mathematical operations, such as addition, subtraction, and logarithm, while leaf nodes represent constants or variables. Due to its tree structure, it is particularly suitable for performing sequential decision-making. This structure, visually depicted in Figure 1.A, facilitates the systematic assembly and analysis of mathematical expressions, especially when their exact forms are initially unknown.

3.3. Symbolic regression as a sequential decision-making task

Symbolic regression involves searching for a sequence $a_{1:T} = a_1, a_2, \dots, a_T$ and constructing it into an expression represented by an expression tree to fit observational data. In this context, a_t represents an operation within a specified search space at time step t .

Previous large-scale transformer-based models approach the symbolic regression problem as a machine translation problem. They use feature extractors on the input data points and then decode the features into expression skeletons in an auto-regressive fashion, which means they produce the entire symbolic tree in a single output. In our study, we reinterpret the task of symbolic regression as an Markov decision process (MDP). An MDP is defined by the tuple (S, A, r, P, ρ) , where S denotes the set of states that accurately represent the current situation, A is the set of possible actions, $r(s, a)$ is the reward function, $P(s'|s, a)$ describes the transition probabilities, and $\rho(s)$ is the initial state distribution.

At each time step t , the model selects an action a_t based on the policy $\pi_\theta(a_t|s_t)$, with s_t being the current state. This state encapsulates both the observed data points (X, y) and the encoded structure of the current tree, derived from previous actions $a_{1:t-1}$. The action a_t is chosen to determine the next operation in the sequence. The symbolic expression $a_{1:T} = a_1, a_2, \dots, a_T$ is then constructed as a trajectory of the MDP, represented as $\tau = s_1, a_1, s_2, a_2, \dots, s_T, a_T$. In our model, rewards are granted only at the termination state, with all other states receiving a reward of 0. This approach is consistent with strategies used in other domains such as various games (Silver et al., 2017; 2016), and robotics (Vecerik et al., 2017; Riedmiller et al., 2018). As a reward measure, we utilize the coefficient of determination (R^2) (Glantz et al., 2001), although it is not the only option for this task. The R^2 is defined as:

$$R^2 = 1 - \frac{\sum_{i=1}^n (y_i - \hat{y}_i)^2}{\sum_{i=1}^n (y_i - \bar{y})^2}, \quad (1)$$

where y_i and \hat{y}_i represent the ground-truth and predicted values for point i , respectively. \bar{y} is the average of the y_i

values across all data points, and n denotes the number of observed data points.

Under the introduced MDP formulation, the goal of an RL-based agent is to find a policy π that maximizes the cumulative reward $J(\pi)$:

$$J(\pi) = \mathbb{E}_{\tau \sim \rho_\pi} \sum_{t=0}^{\infty} r(s_t, a_t). \quad (2)$$

Online RL algorithms require extensive trial and error to decipher the rules of symbolic regression. This task is particularly challenging as it targets only optimal solutions, with all sub-optimal solutions receiving significantly lower rewards. The sparsity of the optimal reward signal exacerbates the inefficiency of searching. Offline RL offers a learning paradigm that merges the ability of supervised learning to leverage existing data with RL’s capacity to optimize arbitrary rewards and leverage temporal compositionality (Levine et al., 2020; Kostrikov et al., 2021; Kumar et al., 2020; Janner et al., 2021). For offline RL, while the ultimate objective remains the optimization of the function specified in Equation 2, there is a fundamental change: the agent is unable to interact directly with the environment or collect new transitions through the behavior policy. Instead, the learning process relies on a predetermined, static dataset of transitions denoted as $D = (s_t^i, a_t^i, s_{t+1}^i, r_t^i)$. This dataset replaces real-time interaction, serving as the primary source for the learning algorithm.

3.4. Symbolic Q-network

Sym-Q is specifically designed to enable sequential decision-making and efficient step-wise updates with online and offline data. It comprises three integral modules:

1. Point set encoder $E_\phi^{points}(X, y)$ which transforms the point sets $(X, y) = ((x_1^1, x_1^2, y_1), (x_2^1, x_2^2, y_2), \dots, (x_n^1, x_n^2, y_n))$ associated with each equation into a latent space, resulting in a fixed-size latent representation denoted as $z^p \in \mathbb{R}^{1 \times K_p}$, where K_p indicates the dimension of the latent variable;
2. Expression tree encoder $E_\psi^{tree}(M_t)$ which maps the current tree’s one-hot encoded matrix M_t into another fixed-size latent representation $z^t \in \mathbb{R}^{1 \times K_t}$, where K_t indicates the dimension of the variable;
3. Q-network $Q_\theta(s_t)$ which is responsible for calculating the Q-value for each potential operation, given the combined latent state $s_t = (z^p, z^t)$.

This structure enables Sym-Q to approach symbolic regression in a novel and efficient way. The overall framework of Sym-Q is depicted in Figure 1. For further details of

the neural network architectures and hyperparameters used, please refer to Appendix B.

3.5. Efficient conservative offline Q-learning for symbolic regression

In training the Sym-Q through offline RL, a significant challenge is the overestimation of values due to distributional shifts between the dataset and the learned policy. To address this, we adopt Conservative Q-learning (CQL) (Kumar et al., 2020), which minimizes the values of state-action pairs outside the training data distribution, while simultaneously maximizing the values within this distribution. Given the sparse reward structure of symbolic regression, where rewards are typically given only at the completion of each trajectory and most sub-optimal trajectories receive lower rewards, we have adapted CQL to this context. Our modified version of CQL is customized for symbolic regression, aiming to effectively leverage optimal offline data in this domain:

$$J(\theta, \psi) = -\mathbb{E}_{(s, a^i) \sim \mathcal{D}} \left[\log \left(\frac{e^{Q_{\theta, \psi}(s, a^i)}}{\sum_{j=1}^m e^{Q_{\theta, \psi}(s, a^j)}} \right) \right], \quad (3)$$

where $Q_{\theta, \psi}$ represents the network and its weight parameters, including those beyond the points encoder. \mathcal{D} represents the training dataset, a^i is the action demonstrated at state s , and $a^j | j \neq i, 1 \leq j \leq m$ are the non-demonstrated actions, regarded as suboptimal.

Building on the relationship between conservative Q-learning loss and cross-entropy loss, our proposed objective function represents the log probability of the optimal action. This mirrors the emphasis of cross-entropy on identifying the correct class. The inclusion of the softmax function in the denominator serves to normalize the Q values across all possible actions, effectively converting them into a probability distribution.

By adopting this objective function, our approach more closely aligns with the principles of traditional supervised learning. This alignment could make the approach more intuitive and straightforward to implement, particularly in scenarios where the correct action at each state is well-defined, such as in symbolic regression. A detailed explanation of the algorithm can be found in Appendix C.

3.6. Supervised contrastive learning for points encoder

Following a similar idea to Li et al. (2022), we implemented the supervised contrastive loss for expressions and data points that share the same skeleton. This approach uses the skeleton of expressions as category labels to enrich supervisory information. More specifically, expressions and their corresponding latent points encoding z_i^p , which belong to the same skeleton, are grouped together in the embedding

space. At the same time, we ensure that the latent points encoding z_j^p from different skeletons are distanced from each other. The supervised contrastive loss is defined as:

$$J(\phi) = \sum_{i=1}^N \frac{-1}{|\mathcal{P}(i)|} \sum_{p \in \mathcal{P}(i)} \log \frac{\exp(E_{\phi}^{\text{points}}(X, y)^i \cdot E_{\phi}^{\text{points}}(X, y)^p / \tau)}{\sum_{j=1}^N \mathbb{1}_{[j \neq i]} \exp(E_{\phi}^{\text{points}}(X, y)^i \cdot E_{\phi}^{\text{points}}(X, y)^j / \tau)}, \quad (4)$$

where $\mathcal{P}(i)$ represents the set of indices for all positives in the multiviewed batch distinct from i , and $|\mathcal{P}(i)|$ is its cardinality; τ is an adjustable scalar temperature parameter controlling class separation; N represents the mini-batch size; $z_i^p = E_{\phi}^{\text{points}}(X, y)^i$ is the points embedding of the sample i in a batch, $z_p^p = E_{\phi}^{\text{points}}(X, y)^p$ is the points embedding of a positive sample sharing the same skeleton as sample i . The overall loss is then given by:

$$J(\phi, \theta, \psi) = J(\theta, \psi) + \alpha J(\phi), \quad (5)$$

where α is a scalar weighting hyperparameter tuned during the training stage. More details about the parameters settings and network architectures can be found in Appendix B.

3.7. Online searching and updating

Acknowledging the limitations in current approaches, it becomes evident that a well-generalized model capable of discovering any possible equation would require an impractically large training dataset, making it infeasible for real-world applications. Therefore, a more practical solution lies in developing a pretrained model that is able to conduct efficient and effective online searches when faced with new formulas. In line with this idea, we propose to build on the offline reinforcement learning objective function detailed in Equation 5 and introduce an off-policy risk-seeking REINFORCE method. This method, inspired by DSO (Petersen et al., 2019), focuses on maximizing best-case performance and setting aside less optimal scenarios. Such a strategy is not only pragmatic but has also been proven effective in enhancing the adaptability and responsiveness of models in the realm of symbolic regression:

$$J(\theta) = -\mathbb{E}_{(s, a^i, R_{\tau}) \sim M} (R_{\tau} - \beta R^*) \log \left(\frac{e^{Q_{\theta}(s, a^i)}}{\sum_{j=1}^m e^{Q_{\theta}(s, a^j)}} \right), \quad (6)$$

where R_{τ} is the online cumulative reward of the corresponding Markov tuple, R^* is the highest cumulative reward during searching, β controls the performance threshold of considered cases, and M is the memory buffer during online searching. Equation (5) is a special case that the $R_{\tau} = 1$.

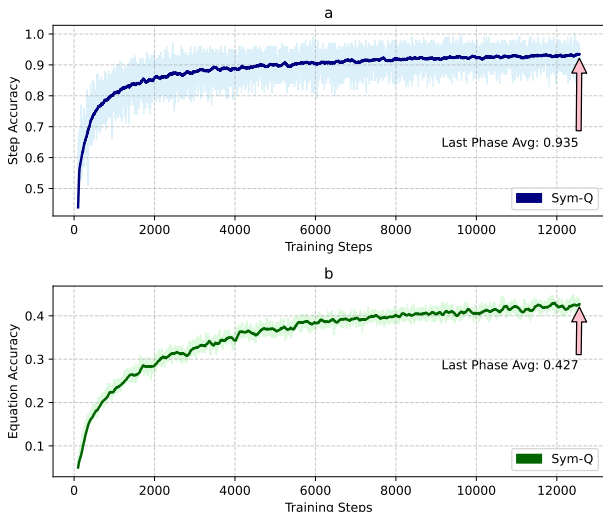


Figure 2. Training curves. These two figures demonstrate the progression of both step accuracy (a) and equation accuracy throughout the training process (b). The x-axis represents the training steps, while the y-axis represents step accuracy and equation accuracy, respectively. The curves have been smoothed using a moving average to facilitate a clearer interpretation of trends.

For the online searching strategy, we simply sample the action based on normalized value distribution.

3.8. Optimization of the coefficients

The BFGS optimization algorithm, commonly used in previous research for calculating coefficients within the skeleton of derived equations, is also employed in our approach, as outlined by Li et al. (2022).

4. Experimental Results

4.1. Training datasets

For our training dataset, we created 5 million mathematical expressions derived from 100,000 pre-defined expression skeletons featuring up to two independent variables (i.e., $d = 2$ and $y = f(x_1, x_2)$), following the guidelines provided by Li et al. (2022). These 100,000 skeletons were generated using the method described by Lample & Charton (2019), which involves constructing a random unary-binary tree and filling its nodes with operators and its leaves with independent variables or constants. We then varied the constant values in each expression 50 times and sampled 100 random data points from each expression, adhering to the procedure outlined in Li et al. (2022). More details about the dataset and the corresponding action space can be found in Appendix D.

4.2. Agent training

We trained the agent using the offline RL algorithm outlined in Section 3. During the training, the agent demonstrated notable improvements in performance, as indicated by the step accuracy and equation accuracy metrics, as depicted in Figure 2. The training curves suggest continuous learning by the agent, implying that extending the training duration could potentially yield further enhancements in performance. We train the model on one NVIDIA GeForce RTX 3090.

4.3. Evaluation on benchmark datasets

In this study, our primary focus is on generating accurate expression skeletons, which are crucial part for deriving physical relationships. It is important to recognize that while various combinations of operator terms can yield a high coefficient of determination, this does not inherently assure the precision of the final predictions or the correctness of the ultimate expression (Li et al., 2022). We evaluate the skeleton recovery rate using the challenging test set proposed by Li et al. (2022), which consists of the same skeletons as in the training set but with different numerical coefficients, named SSDNC dataset (Li et al., 2022). SSDNC dataset is currently the most comprehensive dataset, containing 963 unseen equations. Further details about the SSDNC dataset can be found in Appendix D. Our method is compared against three state-of-the-art (SOTA) transformer-based supervised learning methods, SymPointMLP (Li et al., 2022), SymbolicGPT (Valipour et al., 2021), and NeSymReS (Biggio et al., 2021). Our method achieves a notable recovery rate of **42.7%** without the beam search and an impressive **82.3%** with the implementation of the beam search strategy. As detailed in Table 1, our proposed method surpasses the SOTA methods by up to 32.0%. Furthermore, it outperforms these methods in terms of average R^2 , achieving a remarkable score of **0.95135**.

We also achieve superior weighted average R^2 fitting accuracy across five additional well-known benchmarks, including Nguyen (Uy et al., 2011), Constant, Keijzer (Keijzer, 2003), R rationals (Krawiec & Pawlak, 2013), and the AI-Feynman database (Udrescu & Tegmark, 2020). In addition to the three transformer-based as outlined above, we compared with two additional online searching approaches, DSO (Petersen et al., 2019) and the standard GP-based symbolic regression (Koza, 1994). As detailed in the Appendix E, our method outperforms all compared methods with a weighted average R^2 of **0.95044** across these six benchmarks. Since on these benchmarks, the skeleton recovery rate has not been previously reported, our comparison is based solely on the weighted average R^2 . All evaluations and baseline implementation were conducted following the setup of SymPointMLP (Li et al., 2022).

Methods	Recovery rate	R^2
SymbolicGPT	50.3%	0.74087
NeSymRes	63.4%	0.85792
SymPointML	75.2%	0.94782
Ours	82.3%	0.95135

Table 1. Recovery rate of expression skeletons and R^2 on the SS-DNC benchmark. Sym-Q outperforms the state-of-the-art baselines in both skeleton recovery rate and final fitting R^2 value. All models use the beam search strategy with the beam size equaling 128.

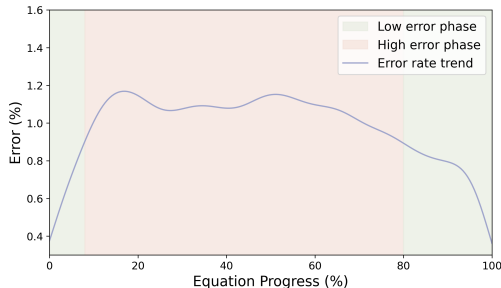


Figure 3. The trend of error rate throughout the expression generation process. The y-axis represents error rates, while the x-axis indicates the progress percentage of the expression generation process, whereby 100% represents a complete equation. A noticeable pattern emerges from this representation: the middle stages of the decision-making process exhibit the highest error rates, while comparatively lower error rates are observed at the beginning and end phases of the process.

5. Analysis of Distinct Properties of Sym-Q

Unlike previous methods that rely solely on transformer decoders, our Sym-Q model uniquely enables step-wise analysis of its decision-making process. This capability not only provides deeper insights into expression generation but also offers a more accurate and detailed metric for evaluating the agent’s performance. In the following, we will explore various aspects of our findings: the error rate trend throughout the expression generation process, the distribution of incorrect selections, and the specific types of errors encountered. All analyses are conducted using the SSDNC dataset. The computation of step-wise accuracy is based on the input of the correct preceding expression tree encoding and the observed data point to determine if the model’s output decision is consistent with the expected decision in the SSDNC dataset. This is done without considering other potential solutions. The overall step accuracy achieved is 93.5%.

The trend of error rate throughout the expression generation process. To account for expressions of different lengths, we normalize them by calculating the percentage of completion. Notably, the highest error rates occur in decisions made during the middle stage of the process, as

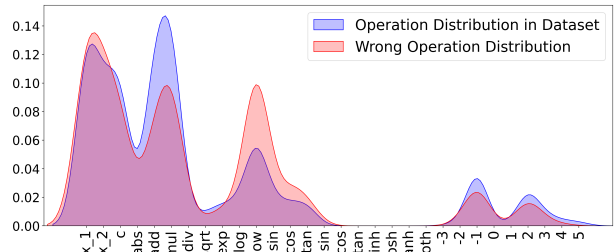


Figure 4. The comparative analysis of two key distributions: the frequency of operations in the training set (blue) and the incidence of incorrect actions (red) encountered in the SSDNC dataset. The y-axis represents error rates, while the x-axis enumerates various operations. There is a notable correlation between these distributions, indicating that the agent tends to favor operations it encountered more frequently during training.

depicted in Figure 3. A potential explanation for this is that initial decisions typically involve binary operations, such as addition (+) and multiplication (\times). These are relatively straightforward, often following a general strategy of expanding the tree at the outset. Conversely, the decisions made towards the end of the process tend to be simpler, as the expression narrows down and becomes more specific.

The distribution of incorrect selections. Our analysis revealed that the frequency of errors closely reflects the distribution of operations in the training set. Specifically, the agent is more inclined to select operations that it encountered more frequently during training. This pattern is clearly illustrated in Figure 4. This finding indicates a potential imbalance in the design of the training set, a consideration that should be addressed in future works.

Analysis of specific error types. We observed that the agent often struggles with determining the exact values of constants. Although it correctly identifies the necessity to include a constant, the chosen value frequently turns out to be incorrect, as illustrated in Figure 5 e) to i). This issue arises because the model does not apply coefficient fitting for constants; instead, it treats each discrete value as a separate action. Additionally, the agent commonly confuses sine and cosine functions. This confusion likely stems from their similar mathematical properties, as shown in Figures 5 c) and d).

Another notable observation concerns the square root operation. The agent often confuses it with the power operation, as illustrated in Figure 5 g). This confusion is somewhat understandable, considering that the square root is equivalent to raising a number to the power of $\frac{1}{2}$. This pattern may suggest that the agent has some grasp of the impact of these operations on mathematical relationships. A similar confusion occurs with the ‘division’ \div operation, which is often mistaken for the ‘power’ operation since ‘division’ is equivalent to ‘power -1’, as shown in Figure 5 a).



Figure 5. Distribution of incorrect decision choices: These charts detail the choices made during instances of incorrect decision-making. Each segment of the pie chart corresponds to an incorrect choice related to a specific correct operation. The size of each segment reflects the proportion of these incorrect choices, with their total sum equaling 1. The title of each chart identifies the correct operation that was targeted in that specific instance.

6. Validation of Online Searching

A significant contribution of our study is the capability of our proposed pretrained model to integrate effectively with online RL methods. We demonstrate that our pretrained model can be seamlessly combined with the online reinforcement learning method described in Section 3.7 to effectively guide the search process. As a case study, we focused on 170 challenging instances within the SSDNC dataset, where the agent fails to correctly recover the skeleton, even with beam search implementation. These instances present substantial challenges for online exploration and learning. It is noteworthy that we limit the agent to a maximum of 50 explorations per search, a number significantly lower than that in other online search methods like DSO (Petersen et al., 2019), which often necessitate over 10,000 searches. We perform the online search for each instance individually. After the online search process, we observe a significant performance improvement in 74.7% of the cases. The initial average R^2 for the 170 cases is 0.328. Remarkably, the average absolute improvement in R^2 for these unsolved expressions is 0.342, a substantial increase of 104.5%. The results are summarised in Table 2.

Moreover, after the online search, the agent successfully uncovers some of underlying skeletons, a significant achievement considering the pretrained Sym-Q’s inability to detect

Methods	R^2
Sym-Q	0.328
Sym-Q + online search	0.670

Table 2. The average R^2 after online search without beam search strategy.

them, even with a 128-size beam search, while the agent accomplishes this with only 50 exploration. For example, in case: $\sin(x_1^2 + x_1x_2 + x_2)$, where the initial output is $\sin(x_2 + x_1^3)$ rewarded 0, the agent uncovers the underlying expression by trying different combinations of x_1 and x_2 to replace term inside the sine function.

7. Discussion and Conclusion

In conclusion, this study marks a significant milestone in the field of symbolic regression. In this work, we innovatively reformulate the symbolic regression as a sequential decision-making task and introduce the Sym-Q model. Sym-Q is trained via our proposed offline RL method and can be also seamlessly combined with online RL approaches. We experimentally demonstrate the effectiveness of this novel problem formulation. Additionally, Sym-Q has the capability to directly derive potential expressions for many unseen equations with high accuracy. Through extensive benchmark evaluations, Sym-Q has been shown to outperform other state-of-the-art algorithms in terms of skeleton recovery rate and to exhibit superior fitting accuracy across most benchmarks. Notably, Sym-Q performs superior performance in recovering the true underlying equations, making it particularly promising for discovering unknown mathematical and physical problems in the future.

Most importantly, the open-source pretrained model we introduce could serve as an effective starting point for more efficient and effective online search. Additionally, we demonstrate for the first time how to integrate this pretrained model with online RL and show its effectiveness in guiding the search process.

A potential future research direction involves designing a more comprehensive dataset that encompasses higher-dimensional expressions, including Ordinary Differential Equations (ODE) and Partial Differential Equations (PDE), for broader pretraining. Additionally, there is still room for optimizing the current MDP formulation. Our current framework represents just the beginning of a promising journey in this field.

Potential Broader Impact

This paper presents work whose goal is to advance the field of Machine Learning. There are many potential societal consequences of our work, none which we feel must be specifically highlighted here.

References

- Augusto, D. A. and Barbosa, H. J. Symbolic regression via genetic programming. In *Proceedings. Vol. 1. Sixth Brazilian symposium on neural networks*, pp. 173–178. IEEE, 2000.
- Bendinelli, T., Biggio, L., and Kamienny, P.-A. Controllable neural symbolic regression. *arXiv preprint arXiv:2304.10336*, 2023.
- Biggio, L., Bendinelli, T., Neitz, A., Lucchi, A., and Parascandolo, G. Neural symbolic regression that scales. In *International Conference on Machine Learning*, pp. 936–945. PMLR, 2021.
- Bladek, I. and Krawiec, K. Solving symbolic regression problems with formal constraints. In *Proceedings of the Genetic and Evolutionary Computation Conference*, pp. 977–984, 2019.
- Devlin, J., Chang, M.-W., Lee, K., and Toutanova, K. Bert: Pre-training of deep bidirectional transformers for language understanding. *arXiv preprint arXiv:1810.04805*, 2018.
- Dubčáková, R. Eureqa: software review, 2011.
- Fletcher, R. *Practical methods of optimization*. John Wiley & Sons, 2000.
- Forrest, S. Genetic algorithms: principles of natural selection applied to computation. *Science*, 261(5123):872–878, 1993.
- Glantz, S. A., Slinker, B. K., and Neilands, T. B. *Primer of applied regression & analysis of variance*, ed, volume 654. McGraw-Hill, Inc., New York, 2001.
- Gustafson, S., Burke, E. K., and Krasnogor, N. On improving genetic programming for symbolic regression. In *2005 IEEE Congress on Evolutionary Computation*, volume 1, pp. 912–919. IEEE, 2005.
- Hendrycks, D. and Gimpel, K. Gaussian error linear units (gelus). *arXiv preprint arXiv:1606.08415*, 2016.
- Hopcroft, J. E., Motwani, R., and Ullman, J. D. Automata theory, languages, and computation. *International Edition*, 24(2):171–183, 2006.
- Janner, M., Li, Q., and Levine, S. Offline reinforcement learning as one big sequence modeling problem. *Advances in neural information processing systems*, 34: 1273–1286, 2021.
- Kamienny, P.-A., d’Ascoli, S., Lample, G., and Charton, F. End-to-end symbolic regression with transformers. *Advances in Neural Information Processing Systems*, 35: 10269–10281, 2022.
- Keijzer, M. Improving symbolic regression with interval arithmetic and linear scaling. In *European Conference on Genetic Programming*, pp. 70–82. Springer, 2003.
- Kostrikov, I., Nair, A., and Levine, S. Offline reinforcement learning with implicit q-learning. *arXiv preprint arXiv:2110.06169*, 2021.
- Koza, J. R. Genetic programming as a means for programming computers by natural selection. *Statistics and computing*, 4:87–112, 1994.
- Krawiec, K. and Pawlak, T. Approximating geometric crossover by semantic backpropagation. In *Proceedings of the 15th annual conference on Genetic and evolutionary computation*, pp. 941–948, 2013.
- Kumar, A., Zhou, A., Tucker, G., and Levine, S. Conservative q-learning for offline reinforcement learning. *Advances in Neural Information Processing Systems*, 33: 1179–1191, 2020.
- Lample, G. and Charton, F. Deep learning for symbolic mathematics. *arXiv preprint arXiv:1912.01412*, 2019.
- Lee, J., Lee, Y., Kim, J., Kosiorek, A., Choi, S., and Teh, Y. W. Set transformer: A framework for attention-based permutation-invariant neural networks. In *International conference on machine learning*, pp. 3744–3753. PMLR, 2019.
- Levine, S., Kumar, A., Tucker, G., and Fu, J. Offline reinforcement learning: Tutorial, review, and perspectives on open problems. *arXiv preprint arXiv:2005.01643*, 2020.
- Li, W., Li, W., Sun, L., Wu, M., Yu, L., Liu, J., Li, Y., and Tian, S. Transformer-based model for symbolic regression via joint supervised learning. In *The Eleventh International Conference on Learning Representations*, 2022.
- Ma, X., Qin, C., You, H., Ran, H., and Fu, Y. Re-thinking network design and local geometry in point cloud: A simple residual mlp framework. *arXiv preprint arXiv:2202.07123*, 2022.
- Matchev, K. T., Matcheva, K., and Roman, A. Analytical modeling of exoplanet transit spectroscopy with dimensional analysis and symbolic regression. *The Astrophysical Journal*, 930(1):33, 2022.

- Mnih, V., Kavukcuoglu, K., Silver, D., Rusu, A. A., Veness, J., Bellemare, M. G., Graves, A., Riedmiller, M., Fidjeland, A. K., Ostrovski, G., et al. Human-level control through deep reinforcement learning. *nature*, 518(7540): 529–533, 2015.
- Mundhenk, T. N., Landajuela, M., Glatt, R., Santiago, C. P., Faissol, D. M., and Petersen, B. K. Symbolic regression via neural-guided genetic programming population seeding. *arXiv preprint arXiv:2111.00053*, 2021.
- Petersen, B. K., Landajuela, M., Mundhenk, T. N., Santiago, C. P., Kim, S. K., and Kim, J. T. Deep symbolic regression: Recovering mathematical expressions from data via risk-seeking policy gradients. *arXiv preprint arXiv:1912.04871*, 2019.
- Riedmiller, M., Hafner, R., Lampe, T., Neunert, M., Degrave, J., Wiele, T., Mnih, V., Heess, N., and Springenberg, J. T. Learning by playing solving sparse reward tasks from scratch. In *International conference on machine learning*, pp. 4344–4353. PMLR, 2018.
- Schmidt, M. and Lipson, H. Distilling free-form natural laws from experimental data. *science*, 324(5923):81–85, 2009.
- Silver, D., Huang, A., Maddison, C. J., Guez, A., Sifre, L., Van Den Driessche, G., Schrittwieser, J., Antonoglou, I., Panneershelvam, V., Lanctot, M., et al. Mastering the game of go with deep neural networks and tree search. *nature*, 529(7587):484–489, 2016.
- Silver, D., Schrittwieser, J., Simonyan, K., Antonoglou, I., Huang, A., Guez, A., Hubert, T., Baker, L., Lai, M., Bolton, A., et al. Mastering the game of go without human knowledge. *nature*, 550(7676):354–359, 2017.
- Tenachi, W., Ibata, R., and Diakogiannis, F. I. Deep symbolic regression for physics guided by units constraints: toward the automated discovery of physical laws. *arXiv preprint arXiv:2303.03192*, 2023.
- Tian, Y., Wang, Q., Huang, Z., Li, W., Dai, D., Yang, M., Wang, J., and Fink, O. Off-policy reinforcement learning for efficient and effective gan architecture search. In *Computer Vision—ECCV 2020: 16th European Conference, Glasgow, UK, August 23–28, 2020, Proceedings, Part VII 16*, pp. 175–192. Springer, 2020.
- Udrescu, S.-M. and Tegmark, M. Ai feynman: A physics-inspired method for symbolic regression. *Science Advances*, 6(16):eaay2631, 2020.
- Uy, N. Q., Hoai, N. X., O’Neill, M., McKay, R. I., and Galván-López, E. Semantically-based crossover in genetic programming: application to real-valued symbolic regression. *Genetic Programming and Evolvable Machines*, 12:91–119, 2011.
- Valipour, M., You, B., Panju, M., and Ghodsi, A. Symbolicgpt: A generative transformer model for symbolic regression. *arXiv preprint arXiv:2106.14131*, 2021.
- Vastl, M., Kulhánek, J., Kubalík, J., Derner, E., and Babuška, R. Symformer: End-to-end symbolic regression using transformer-based architecture. *arXiv preprint arXiv:2205.15764*, 2022.
- Vaswani, A., Shazeer, N., Parmar, N., Uszkoreit, J., Jones, L., Gomez, A. N., Kaiser, Ł., and Polosukhin, I. Attention is all you need. *Advances in neural information processing systems*, 30, 2017.
- Vecerik, M., Hester, T., Scholz, J., Wang, F., Pietquin, O., Piot, B., Heess, N., Rothörl, T., Lampe, T., and Riedmiller, M. Leveraging demonstrations for deep reinforcement learning on robotics problems with sparse rewards. *arXiv preprint arXiv:1707.08817*, 2017.
- Wadekar, D., Thiele, L., Villaescusa-Navarro, F., Hill, J. C., Cranmer, M., Spergel, D. N., Battaglia, N., Anglés-Alcázar, D., Hernquist, L., and Ho, S. Augmenting astrophysical scaling relations with machine learning: application to reducing the sz flux-mass scatter. *arXiv preprint arXiv:2201.01305*, 2022.

A. Pseudo-code for Deployment

We outline the Sym-Q framework in Figure 1. Here we provide the inference pseudo-code in Algorithm 1.

Algorithm 1 Symbolic regression in the test time

Observe the tensor T contains data points
 Initialize the expression tree and the initial one-hot tree matrix M filling with all 0
 Initialize the beam search buffer B with size $2 * L$, and the output buffer OB with size L
while Output buffer not full or beam search buffer emptied **do**
 Sample all the potential actions from $Q_\theta(T, M)$ and put into the beam search buffer B
 Save and update the log probability of the trajectories after appending the new actions
 Rank the trajectories in the beam search buffer B according to the log probability
 Move the terminated trajectories to the output buffer OB
 Keep the top $2 * L$ trajectories in the beam search buffer B
end while
 Performance BFGS for all the trajectories in the output buffer OB and provide the closed-form expressions

B. Neural Networks and Hyperparameters

The Sym-Q consists of four main components: the points encoder, the tree encoder, the fusion layer, and the Q-network. For the **points encoder**, we apply the Set Transformer architecture (Devlin et al., 2018; Biggio et al., 2021), using the original publicly available implementation, which has been proved feasible for large-scale symbolic regression tasks (Biggio et al., 2021; Bendinelli et al., 2023). Referring to the notation of the original paper, our encoder is formed by multiple Induced Set Attention Blocks (ISABs) and one final component performing Pooling by Multihead Attention (PMA), which can reduce the computation burden associated with the self-attention operation. PMA allows us to aggregate the output of the encoder into trainable abstract features representing a compressed representation of the input equation. For the **tree encoder**, we opted for a regular Transformer encoder (Vaswani et al., 2017), using the default PyTorch implementation. In this research, we adopt a fully connected layer of 4096 units as the **fusion layer**. Similarly, for the **Q-network**, we use a fully connected MLP with four hidden layers of 4096 units, predicting the Q-value. GELU activation function (Hendrycks & Gimpel, 2016) is used in all the hidden layers in the fusion layer and Q-network. The other hyper-parameters can be found in Table 3.

C. Efficient Conservative Offline Q-learning

Conservative Q-learning (CQL) (Kumar et al., 2020) addresses the value over-estimation issue in offline reinforcement learning by minimizing the values of state-actions out of the data distribution and maximizing the values over the data distribution. In this work, considering the sparse reward characteristic of symbolic regression, that only the termination of each trajectory can be rewarded and most of the sub-optimal trajectories should be rewarded relatively low, we introduce a modified version of CQL can effectively learn with the optimal offline data:

$$\begin{aligned}
 J(\theta) = & \mathbb{E}_{(s, a^i, s', r) \sim D} \underbrace{\frac{1}{2} [Q_\theta(s_t, a^i) - (r + \gamma \max_{a^*} \hat{Q}_{\hat{\theta}}(s_{t+1}, a^*))]^2}_{\text{term I: TD error}} + \\
 & \underbrace{\frac{1}{2} \mathbb{E}_{a_j | j \neq i, 1 \leq j \leq m} [Q_\theta(s, a^j) - 0]^2}_{\text{term II: conservative Q loss}},
 \end{aligned} \tag{7}$$

where θ is the weight parameters of Q , D is the training dataset, γ is the discounted factor, a^i is the demonstration action at state s , and $a_j | j \neq i, 1 \leq j \leq m$ is the actions not in the demonstration, which can be consider as suboptimal actions. The $\hat{Q}_{\hat{\theta}}$ is the target Q-network that has the same structure as Q but updated through exponentially moving average of the Q weights θ to stabilize the learning (Mnih et al., 2015). As mentioned above, the suboptimal actions mostly can not lead to correct expression and should be rewarded low. Then, the second term, the conservative Q loss, minimize the Q values to 0, the lower bound of this task, which is also similar to the idea of *Risk seeking policy gradient* in DSO (Petersen et al., 2019).

Table 3. Hyperparameters for our models.

Points encoder	
Number of ISABs	5
Hidden dimension	512
Number of heads	8
Number of PMA features	100
Number of inducing points	100
Tree encoder	
Number of layers	5
Hidden dimension	512
Number of heads	8
Training	
Batch size	512
Learning rate	0.0001
Scale weight (w/ CL) α	0.2
Temperature parameter τ	0.07
Max norm of gradients	1.0
Inference	
Beam size	128
Re-start times of BFGS	20

Since the training data, all the demonstrations lead to a perfect recovery of skeleton, $(r + \gamma \max_{a^*} \hat{Q}_{\hat{\theta}}(s_{t+1}, a^*))$ is equal to 1 given discounted factor $\gamma = 1$, which is feasible in this case due to the Q value is bounded between $[0, 1]$. Then we can rewrite the objective function to :

$$\begin{aligned}
 J(\theta) = \mathbb{E}_{(s, a^i) \sim D} & \underbrace{\frac{1}{2} [Q_{\theta}(s, a^i) - 1]^2}_{\text{term I: Q loss}} + \\
 & \underbrace{\frac{1}{2} \mathbb{E}_{a_j | j \neq i, 1 \leq j \leq m} [Q_{\theta}(s, a^j) - 0]^2}_{\text{term II: conservative Q loss}}.
 \end{aligned} \tag{8}$$

The modified objective function can simplify the neural networks without maintaining the target Q-network \hat{Q} . Then, we can further simplify the objective function, and make it very close to multi-class cross-entropy loss in the sense that it emphasizes the correct prediction (or action in this case) while penalizing the others. This simplification is particularly suitable for symbolic regression tasks where the action space is discrete and the optimal action at each state is distinctly defined. Building upon the connection between the conservative Q-learning loss and the cross-entropy loss, we derive the following reformulation:

Maximizing Selected Action’s Q Value: Simplify the first term $\frac{1}{2} [Q_{\theta}(s, a^i) - 1]^2$ of Equation (8) by maximizing $Q_{\theta}(s, a^i)$:

$$\max Q_{\theta}(s, a^i). \tag{9}$$

Normalizing via Softmax Function: Transform Equation (9) to a probabilistic interpretation by applying the softmax function:

$$p(a^i | s) = \frac{e^{Q_{\theta}(s, a^i)}}{\sum_{j=1}^m e^{Q_{\theta}(s, a^j)}}. \tag{10}$$

This inherently manages the Q values of non-selected actions in the second term of Equation (8).

Minimizing Negative Log Probability: Maximize $p(a^i|s)$ by minimizing its negative log:

$$-\log(p(a^i|s_t)) = -\log\left(\frac{e^{Q_\theta(s,a^i)}}{\sum_{j=1}^m e^{Q_\theta(s,a^j)}}\right). \quad (11)$$

New Objective Function: Incorporate the above steps into a new objective function:

$$J(\theta) = -\mathbb{E}_{(s,a^i)\sim\mathcal{D}}\left[\log\left(\frac{e^{Q_\theta(s,a^i)}}{\sum_{j=1}^m e^{Q_\theta(s,a^j)}}\right)\right]. \quad (12)$$

The final objective function represents the log probability of the optimal action, mirroring the focus of cross-entropy on the correct class. The softmax function in the denominator normalizes the Q values across all possible actions, turning them into a probability distribution.

By adopting this modified objective function, our approach aligns more closely with the principles of traditional supervised learning, potentially making it more intuitive and easier to implement, especially in environments where the correct action at each state is clearly defined, such as symbolic regression.

D. Details for Dataset Generation and Action Space

The training set, and SSDNC benchmark are generated following the guidelines provided by Li et al. (2022). We sample each non-leaf node following the unnormalized weighted distribution shown in Table 4. The database approximately contains 100,000 unique expressions’ skeletons. Then the training set is generated by re-sampling 50 numerical constants for each skeleton. The SSDNC benchmark includes approximately 100 unique expression skeletons and 10 re-sampled numerical constants for each skeleton. In this work, at every time step t , we consider 30 different operations, which is listed below in Table 5.

Operation	Mathematical meaning	Unnormalized probability
add	+	10
mul	×	10
sub	−	5
div	÷	5
sqrt	√	4
exp	exp	4
ln	ln	4
sin	sin	4
cos	cos	4
tan	tan	4
pow2	(·) ²	4
pow3	(·) ³	4
pow4	(·) ⁴	2
pow5	(·) ⁵	1

Table 4. Unnormalised probabilities of unary and binary operators used by the dataset generator.

E. Fitting Accuracy on Additional Benchmarks

We evaluate our method and current state-of-the-art approaches on the widely used public benchmarks, including Nguyen benchmark (Uy et al., 2011), the Constant benchmark, the Keijzer benchmark (Keijzer, 2003), R rationals (Krawiec & Pawlak, 2013), the AI-Feynman database (Udrescu & Tegmark, 2020), as well as the SSDNC dataset (Petersen et al., 2019). Nguyen was the main benchmark used in Petersen et al. (2019). In our study, we consider all the expressions with up to two variables. From the results in Table 6, our method outperforms all baseline methods in terms of weighted average R^2 on six benchmarks. The weighted average R^2 is calculated based on the number of expressions in each benchmark. In Table 7-11, we show the name of the benchmark and corresponding expressions.

Operation	Operation id
x_1	0
x_2	1
c	2
abs	3
+	4
*	5
/	6
$\sqrt{\quad}$	7
exp	8
log	9
**	10
sin	11
cos	12
tan	13
\sin^{-1}	14
\cos^{-1}	15
\tan^{-1}	16
sinh	17
cosh	18
tanh	19
coth	20
-3	21
-2	22
-1	23
0	24
1	25
2	26
3	27
4	28
5	29

Table 5. Action space and corresponding id.

Benchmark	Number of expressions	Sym-Q R^2	SymPointMLP R^2	NeSymRes R^2	SymbolicGPT R^2	DSO R^2	GP R^2
Nguyen	12	0.86482	0.99999	0.97538	0.64394	0.99489	0.89019
Constant	8	0.86860	0.99998	0.84935	0.69433	0.99927	0.90842
Keijzer	12	0.94392	0.98320	0.97500	0.59457	0.96928	0.90082
R	3	0.99999	0.99999	0.84935	0.71093	0.97298	0.83198
AI-Feynman	15	0.99975	0.99999	0.99999	0.64682	0.99999	0.92242
SSDNC	963	0.95135	0.94782	0.85792	0.74585	0.93198	0.88913
Weighted avg.	1013	0.95044	0.95020	0.86271	0.74087	0.93483	0.88976

Table 6. Results comparing our Sym-Q with state-of-the-art methods on several benchmarks. All methods use the beam search strategy with the beam size equaling 128. We report the average value of R^2 for each benchmark and the weighted average R^2 on six benchmarks.

Name	Expression
Nguyen-1	$x^3 + x^2 + x$
Nguyen-2	$x^4 + x^3 + x^2 + x$
Nguyen-3	$x^5 + x^4 + x^3 + x^2 + x$
Nguyen-4	$x^6 + x^5 + x^4 + x^3 + x^2 + x$
Nguyen-5	$\sin(x^2) \cos(x) - 1$
Nguyen-6	$\sin(x) + \sin(x + x^2)$
Nguyen-7	$\ln(x) + \ln(x^2 + 1)$
Nguyen-8	\sqrt{x}
Nguyen-9	$\sin(x) + \sin(y)$
Nguyen-9	$\sin(x) + \sin(y)$
Nguyen-10	$2 \sin(x) \cos(y)$
Nguyen-11	x^y
Nguyen-12	$x^4 - x^3 + \frac{1}{2}y^2 - y$

Table 7. Benchmark functions in Nguyen.

Name	Expression
Constant-1	$3.39x^3 + 2.12x^2 + 1.78x$
Constant-2	$\sin(x^2) \cos(x) - 0.75$
Constant-3	$\sin(1.5x) \cos(0.5y)$
Constant-4	$2.7x^y$
Constant-5	$\sqrt{1.23x}$
Constant-6	$x^{0.423}$
Constant-7	$2 \sin(1.3x) \cos(y)$
Constant-8	$\ln(x + 1.4) + \ln(x^2 + 1.3)$

Table 8. Benchmark functions in Constant.

Name	Expression
Keijzer-3	$0.3x \sin(2\pi x)$
Keijzer-4	$x^3 \exp(-x) \cos(x) \sin(x) (\sin(x^2) \cos(x) - 1)$
Keijzer-6	$\frac{x(x+1)}{2}$
Keijzer-7	$\ln x$
Keijzer-8	\sqrt{x}
Keijzer-9	$\ln x + \sqrt{x^2 + 1}$
Keijzer-10	x^y
Keijzer-11	$xy + \sin(x - 1)(y - 1)$
Keijzer-12	$x^4 - x^3 + \frac{y^2}{2} - y$
Keijzer-13	$6 \sin x \cos y$
Keijzer-14	$\frac{8}{2+x^2+y^2}$
Keijzer-15	$\frac{x^3}{5} + \frac{y^3}{2} - y - x$

Table 9. Benchmark functions in Keijzer.

Name	Expression
R-1	$\frac{(x+1)^3}{x^2 - x + 1}$
R-2	$\frac{x^5 - 3x^3 + 1}{x^2 + 1}$
R-3	$\frac{x^6 + x^5}{x^4 + x^3 + x^2 + x}$

Table 10. Benchmark functions in R.

Name	Expression
Feynman-1	$\frac{\exp \frac{-x^2}{2}}{\sqrt{2\pi}}$
Feynman-2	$\frac{\exp \frac{-(xy-1)^2}{2}}{\sqrt{2\pi y}}$
Feynman-3	xy
Feynman-4	xy
Feynman-5	$\frac{1}{2}xy^2$
Feynman-6	$\frac{x}{y}$
Feynman-7	$\frac{\sin x}{\sin y}$
Feynman-8	$\frac{x}{y}$
Feynman-9	$\frac{xy}{2\pi}$
Feynman-10	$1.5xy$
Feynman-11	$\frac{x}{4\pi y^2}$
Feynman-12	$\frac{xy}{x}$
Feynman-13	xy^2
Feynman-14	$\frac{x}{2(1+y)}$
Feynman-15	$\frac{xy}{2\pi}$

Table 11. Benchmark functions in AI-Feynman.